Emirates Journal of Food and Agriculture. 2021. 33(9): 726-741
doi: 10.9755/ejfa.2021.v33.i9.2758
http://www.ejfa.me/

RESEARCH ARTICLE

Screening rice blast-resistant cultivars via synchrotron fourier transform infrared (SR-FTIR) microspectroscopy

Piyaporn Phansak[1]*, Supatcharee Siriwong[2], Rungthip Sangpueak[3], Nantawan Kanawapee[1], Kanjana Thumanu[2], Natthiya Buensanteai[3]

[1]Division of Biology, Faculty of Science, Nakhon Phanom University, Muang Nakhon Phanom, 48000, Thailand, [2]Synchrotron Light Research Institute (Public Organization), Muang Nakhon Ratchasima, 30000, Thailand, [3]School of Crop Production Technology, Institute of Agriculture Technology, Suranaree University of Technology, Muang Nakhon Ratchasima, 30000, Thailand

ABSTRACT

In Asia, one of the most important cereal crops is rice. Presently, a fungal pathogen called rice blast (*Magnaporthe grisea*) is the most devastating diseases affecting this valuable human staple. One of the ways growers can control rice blast is by chemical fungicides; however, the down side to using chemicals is the increase of production cost, environmental contamination, and loss of chemical efficacy over time. The use of resistant rice cultivars provide fungal suppression and have a positive impact on the environment. The objective of this study was to screened rice blast-resistant cultivars via SR-FTIR microspectroscopy and compare it to the traditional method. At 14 days after pathogens inoculation (DAPI) of 80 cultivars and two reference cultivars, the leaves of inoculated plants showed elliptical or spindle-shaped lesions with pointed ends, gray or white centers, and dark-green to reddish-brown margins, with an occasional yellow halo. The results of disease severity were classified as susceptible (17 cultivars), moderately susceptible (28 cultivars), and resistant group (35 cultivars) of all 80 varieties of rice. Rice cultivar no. 34 had the lowest level of disease severity, which was 6.66 ± 11.54%. Furthermore, we evaluated the accumulation of salicylic acid (SA) in rice at 24 DAPI compared with uninoculated plants. The results of the resistant group showed an increase of SA level at 24 DAPI as well as reference resistant cultivars. Rice cultivar no. 34 had SA level of 15.19 μg g^{-1} fresh weight and all other reference-resistant cultivars had a SA level at 14.70 μg g^{-1} fresh weight, respectively. Additionally, screening rice blast-resistant cultivars via SR-FTIR microspectroscopy revealed altered variation in biochemical components of the plants after infection. A comparison of the susceptible, moderately susceptible, and resistant cultivars revealed differences in the biochemical components of rice tissues, which may be correlated with plant defense responses to disease. These outcomes could help breeding programs in terms of the selection of resistant-rice cultivars.

Keywords: Biochemical change; Rice; Rice blast disease; Salicylic acid; SR-FTIR

INTRODUCTION

Rice (*Oryza sativa* L.) is one of the most important cereal crops and is a staple food source worldwide, especially in Asian countries. Asia represents the largest rice production area, which includes the top producing countries such as China, India, Thailand, Cambodia, and Vietnam (Thanh et al., 2017). Rice production worldwide is affected by various biotic and abiotic stressors that are especially important constraints of rice production (Huang et al., 2003). Thus, rice blast, which has been recorded in approximately 85 countries on all continents where rice is cultivated, is considered one of the most damaging rice diseases worldwide. Among all the diseases of rice, rice blast is the most common and most severe in Southeast Asia (Woperieis et al., 2009) and is caused by a nonobligate filamentous ascomycete, *Magnaporthe oryzae* (*Magnaporthe grisea*) (Anamorph = *Pyricularia grisea*). Rice blast is common in all three rice-growing ecosystems: irrigated, rain-fed upland, and lowland area. However, the incidence and severity of this disease are greatest in upland areas.

In India, the total loss due to rice blast from 1960–1961 was 265,000 tons, amounting to approximately 0.8% of the total rice production. However, blast under severe epiphytic conditions can result in 70–90% losses in isolated fields/localities (Devanna et al., 2014; Turaidar et al., 2018; Asibi et al., 2019). Moreover, this disease can cause 70–80% yield losses when predisposing factors, *i.e.*, high mean temperature, greater than 85–89% relative

***Corresponding author:**
Piyaporn Phansak, Division of Biology, Faculty of Science, Nakhon Phanom University, Muang Nakhon Phanom, 48000, Thailand.
Telephone: (+66)885619059. **Fax:** (+66)042503776. **E-mail:** pphansak@npu.ac.th

Received: 31 May 2021; **Accepted:** 25 September 2021

humidity, drought stress, excessive nitrogen fertilization, and the presence of dew (Kwanwah et al., 2020). Ashkani et al. (2015) and Kongcharoen et al. (2020) reported that rice blast can cause yield losses of 30–50% in large rice-producing areas under favorable environmental conditions. In 1992, a severe rice blast epidemic in Thailand in 1992 damaged more than 650,000 tons of rice (equal to 60% of the total rice yield) in most provinces in the northern and northeastern regions (Disthaporn, 1994; Parinthawong et al., 2015; Poonsin and Parinthawong, 2020).

In Thailand, rice blast is controlled by field applications of fungicides, which not only increases cost associated with rice production, but also, the likelihood of chemical contamination of the environment and food crops (Kongcharoen et al., 2020). Therefore, the use of resistant cultivars (host plant resistance) is thought to be one of the most economically efficient and environmentally friendly methods of crop protection (Brzozowski and Mazourek, 2018; Straub et al., 2020). At present, approximately 100 rice blast resistance genes have been identified, among of which, 45% are from *japonica* cultivars, 51% are from *indica* cultivars, and 4% are from wild species of rice (Sharma et al., 2012). Under field conditions, blast resistance tends to be unreliable, with resistance often failing or breaking down which is thought to be due to high-pathogen plasticity in the field causing single-gene resistance to break down after 3–5 years (Lang et al., 2009).

Resistant plant cultivars are important to combating rice blast disease. In plants, there are resistant pathways including gene-for-gene recognition and biochemical mechanisms (Andersen et al., 2018; Wu et al., 2021). Resistant host plants have disease resistance (*R*) genes that trigger defense mechanism events (Dong and Ronald, 2019; Jiang et al., 2020). There is specific recognition between *R* genes of host plants and avirulence (*avr*) genes of pathogens that are responsible for plant defense responses (Forouhar et al., 2005; Petit-Houdenot and Fudal, 2017). Furthermore, plants have biochemical defenses that include both secondary metabolites and phenolic compounds that are produced in cells before or after infection; these defensive compounds tend to play a more important role than do structural defense mechanisms (Isah, 2019; Erb and Kliebenstein, 2020; Bigini et al., 2021).

Salicylic acid (SA) is a secondary metabolite in plants and plays a signaling role in protection against plant pathogens (Filgueiras et al., 2019; Janda et al., 2020; Lefevere et al., 2020). SA is the key signaling molecule involved in several plant defense-response pathways; SA activates various plant defense-related genes such as pathogenesis-related 1 (*PR-1*), peroxidase (*POD*), polyphenol oxidase (*PPO*), superoxide dismutase (*SOD*), and phenylalanine ammonia lyase (*PAL*) and activates various disease resistance mechanisms (Lee et al., 1992; Wu et al., 2019; Lefevere et al., 2020; Thepbandit et al., 2021; Zhang et al., 2021). SA also alters the activity or synthesis of certain enzymes and increases the expression of genes related to defense and to the generation of free radicals (Huang et al., 2019). In rice, SA can play a role as a constitutive defensive compound and affects the lignin precursors p-coumaric and ferulic acid in the induction of disease resistance (Desmedt et al., 2021). Moreover, SA plays a crucial role in systemic acquired resistance (SAR) in rice by upregulating the expression of the *NPR1* gene, ultimately increasing resistance to blast and leaf blight diseases (Backer et al., 2019). SA also induces the accumulation of H_2O_2 in rice, which subsequently stimulates the expression of genes that encode rice pathogenesis-related (PR) proteins associated with the hypersensitive response (HR) (War et al., 2011; Thanh et al., 2017). In addition, SA is a key player involved in NPR1, MPK4, and processes (methylation, amino acid conjugation, and S-nitrosylation) contributing to the conjugation of SA derivatives that both act as signaling molecules and play a role in signaling perception pathways (Li et al., 2019). In addition, SA was shown to be required for the induction of programmed cell death (PCD) inducing infections and defense responses in the Arabidopsis *acd11* mutant (Bernacki et al., 2021; Brodersen et al., 2005). It has also been reported that jasmonic acid (JA) and ethylene (ET) exhibit cross-talk between the SA-dependent and the SA-independent pathways in the activation of multiple resistance mechanisms in various combinations (Li et al., 2019).

Fourier transform infrared (FTIR) microspectroscopy is a technique used for identifying various biochemical components and contents within biological samples (Cao et al., 2017; Buitrago et al., 2018). The principle of this technique is the vibration at various frequencies resulting from the elements and types of bonds that compose biochemical compounds, such as CH_2, CH_3 stretching vibrations of lipids, C=O stretching from pectin and C-H, N-H stretching vibrations of proteins and C-O, C-O-C vibration of cellulose and hemicellulose. FTIR microspectroscopy is nondestructive technique and provide label free on the samples. In addition, it can provide biomolecule with highly sensitive from the sample. While, the conventional technique to study the changes of biomolecule in leaf tissue must require time and cost (Rosi et al., 2019; Durak et al., 2020). This technique is a powerful tool for identifying specific types of chemical bonds within a molecule based on its infrared (IR) absorption spectrum (Lahlali et al., 2016; Gierlinger, 2017).

An even more advanced technology is the SR-FTIR microspectroscopy involves the use of IR light from a

synchrotron radiation source. SR-FTIR microspectroscopy couples the use of an SR-FTIR spectrometer with microscopy and can be applied to quantify the components of unknown samples and to display chemical images. The advantages of synchrotron radiation include a brightness that is greater than a global source and its functionality with aperture sizes smaller than 10 × 10 μm^2, with high signal strength (Thumanu et al., 2017; Dinant et al., 2019). SR-FTIR imaging allows spectroscopic examination with mid-IR wavelengths, encompassing wavenumbers from 400–4000 cm^{-1} (Turker-kaya and Huck, 2017). The resultant chemical images within the samples can be displayed in two or three dimensions in various color scales. The application of SR-FTIR microspectroscopy in conjunction with multivariate analysis can be used to monitor cellular components of biological samples, which has been presented in a number of publications. This technique can be used to explain the variation in cellular components of plant tissues under different conditions or between groups of treatments. Alonso-Simón et al. (2011) used SR-FTIR microspectroscopy to monitor changes in plant cell wall composition after inhibition by cellulose biosynthesis inhibitors (CBIs), and the results were related to abiotic and biotic stresses in plants.

Additionally, this technique can also be used to study plant interactions with a disease or an inducing agent. Using SR-FTIR microspectroscopy, Thanh et al. (2017) studied the biochemical changes in and the defense response of rice plants after induction with SA and inoculation with *Xanthomonas oryzae* pv. *oryzae* (*Xoo*). The authors reported that SA could induce plant defense responses to disease by altering biochemicals inside plant cells, acclimating the plants to protection against disease. Thumanu et al. (2017) successfully applied SR-FTIR microspectroscopy and imaging to identify biochemical and structural changes in chili pepper plants after induction by *Bacillus subtilis* strain D604 and inoculation with an anthracnose-causing fungal pathogen. Thus, SR-FTIR can be used to obtain high-quality images to classify variation in the biocomposition of plant tissue and can be used to explain the defense mechanism of plants in response to infection (Thumanu et al., 2017).

In this study, the rapid screening SR-FTIR microspectroscopy was used to classify disease-resistance cultivars and understand the biomolecule differentiation in plant tissue. Therefore, the goals of this research were to use SR-FTIR combined with multivariate analysis to evaluate the biomolecular components of different groups of rice plants, including those susceptible, moderately susceptible, and resistant to rice blast disease, and to characterize these different groups of rice cultivars before and after inoculation with rice blast.

MATERIALS AND METHODS

Rice materials

Seeds of 80 rice cultivars were obtained from the Sakon Nakhon Rice Research Center, Thailand, and Thai jasmine rice (KDML105) and Leuang Pratew rice seeds were obtained from the Nakhon Ratchasima Rice Seed Center. KDML105 and Leuang Pratew were used as sensitive and resistant reference cultivars, respectively (Table 1). All rice seeds were first soaked in sterilized water overnight. Afterward, the seeds (10 seeds/pot) were grown in clay pots filled with soil collected from the Suranaree University of Technology, and the pots were divided into two groups with respect to *Pyricularia oryzae* pv. *oryzae*: inoculated and uninoculated. Each rice cultivar was replicated three times. The rice plants were grown for 45 days under greenhouse conditions. Fertilizer (N-P-K: 15-15-15) was applied every 7 days after planting (1 g/pot) (Thanh et al., 2017).

Fungus preparation for plant inoculation

A stock culture of *P. oryzae* pv. *oryzae* was obtained from the Plant Protection Research and Development Office, Bangkok, Thailand. The culture was reisolated, maintained on potato dextrose agar (PDA) and stored at 4 °C until use. The fungi were placed on PDA and incubated at 25 °C. After 7 days, the culture was grown under dark/light conditions to induce sporulation until full sporulation occurred (Fig.1a, b). The samples were then diluted with sterilized water and subsequently counted with a hemocytometer, after which they were adjusted to 10^8 spores ml^{-1}. The rice plants were divided into two treatment groups: inoculated and uninoculated. The spore suspensions were sprayed onto rice leaves at 45 days after planting; the non-inoculated plants were sprayed with sterilized water as a control. The rice plants were subsequently covered with a plastic bag to maintain moisture. The plastic bags were removed at 24 hours after inoculation, after which, the rice plants were observed for disease until symptom development (Thanh et al., 2017).

Disease severity assessment

Rice blast disease severity of the leaves was assessed at 14 days after inoculation. The assessment was undertaken by sampling three rice plants per cultivar. The percentage of infected leaf area was rated as one of three categories according to the methods of Haggag et al. (2014). The disease response for each rice plant was evaluated by averaging the disease severity rating derived from individual plants. The disease response indices were as follows: 0 < 25% infected leaf area, resistant; 25 > 75%, moderately susceptible; and > 75%, susceptible (Haggag et al., 2014; Vasudevan et al., 2014).

Endogenous SA analysis

The method described by Raskin et al. (1989) was used for the analysis. Pooled rice leaf tissues (0.5 g) from

Table 1. List of 80 rice cultivars collected from the northeastern part of Thailand.

Cultivar No.	Cultivar Name	Location	Cultivar No.	Cultivar Name	Location
1	Doi Won	Mukdahan	41	Jao-Rein-Thong	Udon Thani
2	E-Tum	Sakon Nakhon	42	Kee-Tom-Pun	Udon Thani
3	Mae-Peung	Mukdahan	43	Kao-Sa-Mart	Kalasin
4	E-Kao	Sakon Nakhon	44	Rark-Phai	Sakon Nakhon
5	Pao-Mia	Mukdahan	45	Leb-Mar	Sakon Nakhon
6	Lao-Tak	Sakon Nakhon	46	Kee-Thom	Sakon Nakhon
7	Pra-In	Nakhon Phanom	47	Kab-Mark	Sakon Nakhon
8	San-Pa-Tong-Door	Nakhon Phanom	48	Kan-Tarn	Sakon Nakhon
9	Khao-Kam	Mukdahan	49	Hang-Nark	Sakon Nakhon
10	Jao-Deang	Sakon Nakhon	50	Kan-Tarn	Sakon Nakhon
11	Lhong-Ma	Mukdahan	51	E-Tam	Sakon Nakhon
12	Tab-Mouy- Kao	Sakon Nakhon	52	Hom-Thung	Sakon Nakhon
13	Luang-Khaew	Nakhon Phanom	53	Mark-Yom	Loei
14	Ma-Yom	Sakon Nakhon	54	Khao-Haw	Sakon Nakhon
15	Hom-Door	Mukdahan	55	Ka-set-Door	Sakon Nakhon
16	Hang-Yee	Sakon Nakhon	56	Hom-Nang-Nuan	Kalasin
17	Kham-Phai	Sakon Nahon	57	Hom-Heud	Sakon Nakhon
18	E-Khew-Non-Tung	Mukdahan	58	Hom-Dor	Sakon Nakhon
19	Door-Deang	Sakon Nakhon	59	Hom-Nang-Nuan	Nakhon Phanom
20	Nheaw-Jao (PW6060-22-373)	Sakon Nakhon	60	Kao-Hom	Nakhon Ratchasima
21	Khab-Yang	Sakon Nakhon	61	Hom-Nang-Nuan	Sakon Nakhon
22	Luang-Yai 75-4-62	Sakon Nakhon	62	Hom-Pae	Khon Kaen
23	Nang-Whan 60-7-91	Sakon Nakhon	63	Hom-Suan	Kamphaengpet
24	Hang-Yee 563-2-20	Sakon Nakhon	64	Kee-Tom-Dam	Sakon Nakhon
25	Khee-Tom-Dam	Sakon Nakhon	65	Leb-Ma	Sakon Nakhon
26	Nang-Suan	Sakon Nakhon	66	E-Deang-Noi	Sakon Nakhon
27	Mark-Bid	Sakon Nakhon	67	Sam-Ruang	Sakon Nakhon
28	Jao-Sam-Deuan	Nakhon Ratchasima	68	Kra-dard	Sakon Nakhon
29	Hin-Son	Nakhon Ratchasima	69	Sam-Deuan-Hang	Nakhon Phanom
30	Khao-Hom	Petchaboon	70	Luang-Boon-Ma	Udon Thani
31	Luang-Thong	Udon Thani	71	Jao-Door	Nongbualamphu
32	Kee-Tom-Hang-Nark	Udon Thani	72	Do-Yuan	Nongbualamphu
33	E-Lhong-Ma	Udon Thani	73	Khaen-Pra-Doo	Sukhothai
34	Pa-Ma	Udon Thani	74	Door-Noi	Yasothon
35	Hang-Yee 3908	Sakon Nakhon	75	E-Tok	Yasothon
36	Jao-Khao	Udon Thani	76	Khao-Soi	Kalasin
37	Kee-Tom-Nark	Udon Thani	77	Door-Sa-Kon	Yasothon
38	Jao-Loy	Udon Thani	78	Ma-Fai	Sakon Nakhon
39	Tom-Door	Udon Thani	79	Ma-Prang	Sakon Nakhon
40	Khao-Yai	Udon Thani	80	E-Tang	Sakon Nakhon

each replication were randomly sampled, frozen in liquid nitrogen, and macerated in a cold mortar with 1 mL of extraction solution (90:9:1 absolute methanol: glacial acetic acid: distilled water [v/v/v]). The extract was subsequently centrifuged at 12000 rpm at 4 °C for 15 min, and the supernatant was collected for analysis. To measure the SA content, 500 µL of the supernatant and an equal volume of 0.02 M ferric ammonium sulfate were mixed together and incubated at 30 °C for 5 min, after which the absorbance at 530 nm was read by a spectrophotometer (BioTek™ Epoch™ Microplate Spectrophotometer, USA). To determine the actual amount of SA in the sample, the absorbance was compared with that of the reference standard.

The data concerning the SA content of the samples of three replications per treatment at 24 hours after inoculation were subjected to a one-way analysis of variance (ANOVA) separately via SPSS 14. Duncan's new multiple range test (DMRT) was used to separate the treatment means at≤ 0.05.

SR-FTIR microspectroscopy imaging analysis

Sample preparation

Rice leaves were collected from three fungal inoculation groups that corresponded to three disease severities [susceptible (SUS), moderately susceptible (MOD), and tolerant (TOL)] and were compared with rice leaves collected from the uninoculated group. KDML105 and

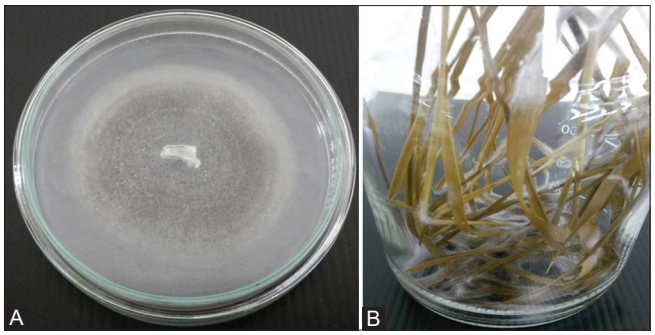

Fig 1. Fungus preparation for plant inoculation A *P. oryzae* pv. *oryzae* on potato dextrose agar (PDA) and stored at 4°C. B The culture was grown under dark/light conditions to induce sporulation until full sporulation occurred.

Leung Pratew served as sensitive (SENT) and resistant (RES) references (controls), respectively. Leaf samples were collected at 7 days after inoculation. The rice leaves were then cut into pieces that were 1 × 1 cm^2 in size, embedded in optimal cutting temperature (OCT) compound and then frozen immediately in liquid nitrogen. The OCT compound was used to avoid causing freezing damage to the samples. The samples were stored at –80 °C until their use for sectioning. The rice leaves were cross-sectioned to 7 μm via a Microm™ HM 525 Cryostat at –22 °C. The samples were subsequently put on transparent IR 2-mm-thick BaF_2 windows and stored in a desiccator before use (Thanh et al., 2017; Thepbandit et al., 2021).

SR-FTIR microspectroscopy analysis

The spectral data were measured with an IR microspectroscopy beamline (BL4.1 IR Spectroscopy and Imaging) at the Synchrotron Light Research Institute (SLRI). The spectra were acquired with a Vertex 70 FTIR spectrometer (Bruker Optics, Ettlingen, Germany) coupled to an IR microscope (Hyperion 2000, Bruker Optics) that was equipped with a liquid nitrogen-cooled mercury cadmium telluride (MCT) detector (100 μm in size). The spectra were collected over the mapping area in transmission mode from 4000–600 cm^{-1}, at a spectral resolution of 4 cm^{-1}, and with an aperture size of 10 × 10 μm^2. Sixty-four scans were collected for the background, and the background spectrum of barium fluoride (BaF_2) windows was recorded before each sample measurement (Thanh et al., 2017).

Data processing for image analysis

The IR image of each sample was analyzed by CytoSpec v.1.3 (CytoSpec Inc., NY, USA). The spectra were transformed to second-derivative spectra via 13 smoothing points and were vector normalized to normalize the effects of different sample thicknesses. A cluster analysis was performed, and the results were color coded for each class on the basis of the spectral features of the different biochemicals within the rice leaf tissues between clusters. The outputs of hierarchical cluster analysis (HCA) were visualized as dendrograms, with a unique color assigned to each spectral cluster (Pei et al., 2018; Straková et al., 2020).

Principal component analysis (PCA)

The spectra of each sample group were analyzed via PCA. The data were preprocessed by taking the second derivative and then normalized using extended multiplicative signal correction by the use of the spectral regions from 3000–2800 cm^{-1} and 1800–900 cm^{-1} via UnscramblerX 10.5 software (CAMO, Oslo, Norway) (Staniszewska-Ślęzak et al., 2015; Goff et al., 2019).

Hierarchical cluster analysis (HCA)

HCA was performed on the second derivatice-transformed spectra via Ward's algorithm, which uses a matrix-defining interspectral distance to identify the most similar IR spectra. Spectral distances were subsequently calculated as D-values (Pei et al., 2018).

RESULTS

Disease severity assessment

The 80 rice cultivars and two reference cultivars were inoculated with *P. oryzae* pv. *oryzae* and were subsequently rated for their disease severity. The rice blast severity was compared between the treatment and the control group (Table 2 and Table 3). At 14 days after inoculation, the rice leaves started to show elliptical or spindle-shaped lesions that had pointed ends and gray or white centers; moreover, the leaves had dark-green to reddish-brown margins, sometimes with a yellow halo (Fig. 2a, b). In general, in cases of severe infection, leaf sheaths can dry up, and whole plants can die; severely infected fields have a scorched appearance. In the present study, hypersensitive spots or small, round-to-elliptical brown lesions formed on the resistant rice cultivars.

Compared with the susceptible rice cultivar KDML105 and the resistant rice cultivar Leuang Pratew, which exhibited 66.66% and 33.33% rice blast severity, respectively, 17 rice cultivars showed severe rice blast disease (53.33–93.33% disease severity), 28 rice cultivars showed moderate disease severity (40.00–50.00% disease severity), and 30 rice cultivars showed less than 35% rice blast severity. The results of this study, therefore, led to the classification of three resistance levels on the basis of disease severity: susceptible, moderately susceptible, and resistant cultivars (Rijal et al., 2017; Loladze et al., 2019).

Endogenous SA analysis

The accumulation of SA in the 80 rice cultivars with different levels of resistance at 24 hours after inoculation with *P. oryzae* pv. *oryzae* was compared with that in the

Table 2. Disease severity scores of representative rice (*Oryza sativa*) samples with rice blast disease caused by *Pyricularia oryzae* pv. *oryzae* obtained from Thailand.

Cultivar No.	Rice blast disease severity (%)	Resistant level*	Cultivar No.	Rice blast disease severity (%)	Resistant level*
1	20.00 ± 0.00 hijkl	R	22	40.00 ± 0.00 cdefghijk	M
2	56.66 ± 30.55 bcdef	S	23	66.66 ± 23.09 abc	S
3	43.33 ± 28.86 cdefghij	M	24	26.66 ± 15.27 fijkl	R
4	23.33 ± 5.77 ghijkl	R	25	33.33 ± 11.54 defghijkl	R
5	16.66 ± 15.27 ijkl	R	26	33.33 ± 11.54 defghijkl	R
6	10.00 ± 10.00 kl	R*	27	33.33 ± 11.54 defghijkl	R
7	53.33 ± 15.27 bcdefg	S	28	40.00 ± 0.00 cdefghijk	M
8	40.00 ± 40.00 cdefghijk	M	29	53.33 ± 11.54 bcdefg	S
9	46.66 ± 5.77 cdefghi	M	30	40.00 ± 0.00 cdefghijk	M
10	26.66 ± 11.54 fijkl	R	31	80.00 ± 0.00 ab	S*
11	46.66 ± 15.27cdefghi	M	32	33.33 ± 11.54 defghijkl	R
12	26.66 ± 11.54 fijkl	R	33	40.00 ± 0.00 cdefghijk	M
13	16.66 ± 5.77 ijkl	R	34	6.66 ± 11.54 l	R**
14	26.66 ± 5.77 fijkl	R	35	40.00 ± 20.00 cdefghijk	M
15	30.00 ± 10.00 efghijkl	R	36	80.00 ± 0.00 ab	S*
16	13.33 ± 11.54 jkl	R	37	53.33 ± 11.54 bcdefg	S
17	40.00 ± 0.00 cdefghijk	M	38	33.33 ± 11.54 defghijkl	R
18	43.33 ± 5.77 cdefghij	M	39	46.66 ± 11.54 cdefghi	M
19	63.33 ± 5.77 bcd	S	40	66.66 ± 11.54 abc	S
20	26.66 ± 5.77 fijkl	R	41	46.66 ± 11.54 cdefghi	M
21	40.00 ± 0.00 cdefghijk	M	42	26.66 ± 11.54 fijkl	R

Table 3. Disease severity scores of representative rice (*Oryza sativa*) samples with rice blast disease caused by *Pyricularia oryzae* pv. *oryzae* strains obtained from Thailand separated by groups.

Resistant level	Rice blast disease severity (%)	Cultivar No.	Total
Resistant	0–39	1, 4, 5, 6, 10, 12, 13, 14, 15, 16, 20, 24, 25, 26, 27, 32, 34, 38, 42, 43, 52, 54, 55, 57, 60, 61, 62, 69, 71, 72, 74, 75, 77, 78, 79	35
Moderately susceptible	40–50	3, 8, 9, 11, 17, 18, 21, 22, 28, 30, 33, 35, 39, 41, 44, 45, 47, 49, 50, 51, 58, 59, 66, 67, 70, 73, 76, 80	28
Susceptible	51–100	2, 7, 19, 23, 29, 31, 36, 37, 40, 46, 48, 53, 56, 63, 64, 65, 68	17

uninoculated control cultivars. The results showed that the uninoculated 80 rice cultivars had significantly different levels of basal SA levels (data not shown). Therefore, the selection of cultivars that are resistant, moderately susceptible, and susceptible in terms of rice blast disease severity was based on the findings of previous experiments. As such, the accumulation of SA in 20 rice cultivars with different levels of resistance at 24 hours after inoculation with *P. oryzae* pv. *oryzae* was compared with that in the uninoculated control cultivars. The results showed that the 20 uninoculated rice cultivars also had significantly different levels of basal SA levels (Table 4 and Fig. 3). Moreover, uninoculated Leuang Pratew (resistant cultivar) and rice No. 31 had the greatest SA accumulation (14.69 and 14.68 $\mu g\ g^{-1}$ fresh weight, respectively), followed by rice No. 23, with 14.62 $\mu g\ g^{-1}$ fresh weight. In the inoculated treatment, the SA accumulation significantly differed between nearly all the resistant and moderately susceptible rice cultivars (Table 4 and Fig. 3). Rice Nos. 3, 16, and 13 presented the greatest accumulation of SA—16.90, 16.59 and 16.34 $\mu g\ g^{-1}$ fresh weight, respectively. Together, these results indicated that the SA signaling pathway plays a crucial role in rice immunity against pathogen infection in the SAR of resistant and moderately susceptible rice cultivars.

SR-FTIR microspectroscopy analysis

SR-FTIR images were processed with CytoSpec software to create images of leaf samples. In each image, the rice leaf structure was separated on the basis of the composition of the epidermis, mesophyll, and vascular bundles and on the basis of the characteristics of the spectra or biochemical components, including lipids, protein, pectin, lignin, cellulose, and hemicellulose (Fig. 4). The spectra of the mesophyll layer of the rice leaves were analyzed via Unscrambler X 10.5 software (CAMO, Oslo, Norway) to classify the inoculated rice leaves and the uninoculated rice leaves. Figs. 5–7 show the results of the PCA and loading plots of the leaves of the susceptible, moderately susceptible, and tolerant groups of rice plants after

Table 4. Salicylic acid (SA) accumulation level (μg g^{-1} fresh weight) in 20 rice (*Oryza sativa*) cultivars not inoculated or inoculated with *Pyricularia oryzae* pv. *oryzae* at 24 hours after inoculation under greenhouse conditions.

Resistant	Cultivar No.	Uninoculated	24 hours after inoculation
	5	14.1438 ijklm	15.82678875 cdefg
	6	14.0251125 ijk	15.3417525 fghij
	13	13.9533725 k	16.34031 bc
	16	14.1759775 fijk	16.59271875 ab
	34	14.1685925 fijkl	15.19537125 hijk
	57	14.520435 abc	15.5063325 defgh
	60	14.292555 defg	15.32751 fghij
	T	14.6939825 a	14.7034775 klmn
Moderately susceptible	3	13.990825 ijk	16.906845 a
	9	14.0704775 jklm	15.2309775 ghijk
	11	13.963395 jk	16.10214375 bcde
	41	14.3046875 defg	15.86951625 cdef
	45	14.526765 abc	15.81096375 cdefg
	59	14.049905 jklm	15.01338375 ijkl
	80	14.24719 defgh	16.31736375 bcd
Susceptible	23	14.6285725 ab	14.41177 lmn
	31	14.6897625 a	14.46241 lmn
	36	14.389615 cde	14.3511075 mn
	40	14.45186 bcd	14.1886375 n
	48	14.36746 cdef	14.946655 lkjm
	56	13.9480975 k	15.53244375 defgh
	S	14.18811 efghi	15.72867375 defgh
	CV %	1.70	4.88
	F-test	**	**

Table 5. Band assignments of the Fourier transform infrared (FTIR) spectra of plants (Thanh *et al.* 2017; Thumanu *et al.* 2017)

Wavenumber (cm^{-1})	Functional groups
1730	C=O ester of lignin and pectin
1700–1600	Amide I components resulting from the stretching of C=O and C-N and the N-H bending from antiparallel pleated sheets and β-turns of proteins
1600–1500	Amide II resulting from N-H bending and C-N stretching
1513	C=C aromatic skeleton vibration from lignin
1470	Asymmetric CH_2 and CH_3 bending from lipids
1340	Symmetric CH_2 and CH_3 bending from lipids
1240	C=O stretching of hemicellulose and lignin
1200–1000	C-O-C glycoside ether mainly from hemicellulose and polysaccharides

inoculation compared with no inoculation; PCA is the most common multivariate technique for breaking down a data matrix and concentrating the source of variability within the data into the first few principal components (PCs). Scatter plots of each group of rice leaves are PC1 and PC2. These results indicate that the inoculated and uninoculated rice leaves could be separated by the first 2 PCs. The separation between PC1 and PC2 corresponded to a total variance of 28% from PC1 and 16% from PC2 for the susceptible group, 38% from PC1 and 17% from PC2 for the moderately susceptible group, and 47% from PC1 and 12% from PC2 for the tolerant group. The clear separation revealed by the PCA showed the relatively strong distinction between the uninoculated and inoculated groups, which indicated that the chemical composition of the uninoculated rice leaves and inoculated rice leaves differed. These results corresponded with those of the HCA (Figs. 5d, 6d, and 7d), which revealed that the inoculated and uninoculated groups of rice leaves could be separated into two groups on branches B and D. Average spectral plots based on the PCA data of the rice leaves are shown in Figs. 5c, 6c, and 7c. To compare the different spectra between the two groups (inoculated and uninoculated), the averages of the second derivative-transformed spectra were preprocessed. Spectral changes in the cellulose and hemicellulose region (1200–1250 cm^{-1}) and polysaccharide region (1200–900 cm^{-1}) were observed in the group of susceptible rice leaves after inoculation. However, the spectral changes in the moderately susceptible group indicated that the spectral ranges in the regions corresponding to polysaccharides (1200–900 cm^{-1}), protein (1700–1600 cm^{-1}), cellulose and hemicellulose (1200–1250 cm^{-1}), and pectin (1740–1700 cm^{-1}) increased after inoculation. Spectral changes in the tolerant rice leaves after inoculation occurred in the region corresponding to protein (1700–1600 cm^{-1}), while the uninoculated group of tolerant rice leaves showed a high intensity that corresponded to the pectin (1737 cm^{-1}), lignin (1517 cm^{-1}), and polysaccharide (1200–1250 cm^{-1}) regions.

Figures 8 and 9 show the PCA, average spectra, and HCA results of the inoculated and uninoculated groups of the susceptible, moderately susceptible, and tolerant cultivars. The scatter plots based on the PCA revealed clear separation between the inoculated and uninoculated groups. The uninoculated group of susceptible plants exhibited a major spectral peak within the polysaccharide region, while peaks within the spectral regions corresponding to protein (1658 cm^{-1} and 1548 cm^{-1}), lignin (1517 cm^{-1}), and pectin (1740 cm^{-1}) were observed in the moderately susceptible and tolerant plants. However, after inoculation, the intensity of the spectral region corresponding to polysaccharides in the susceptible rice leaves was greater than that in the other groups. The inoculated groups of moderately susceptible and tolerant plants presented distinct spectral regions corresponding to protein, lignin, and pectin. The results of the HCA dendrogram of the average spectra after inoculation corresponded to those of the PCA scatter plots of the group of susceptible rice leaves, which was separated from the other groups.

When the spectra were compared with those of the reference controls of the sensitive and resistant rice leaves, the PCA results revealed clear separation between the groups of rice leaves, which corresponded to the results of the HCA. The HCA revealed clear separation between the resistant group of rice leaves and the susceptible group after inoculation (Fig. 10d). The average spectra of uninoculated plants indicated that the major spectral region corresponding to pectin differed between the resistant group of rice leaves and the tolerant group of rice leaves, while the spectral regions corresponding to polysaccharides and protein differed between the susceptible group of rice leaves and the sensitive group of rice leaves (reference cultivar KDML105). However, after inoculation with *P. oryzae* pv. *oryzae*, the region corresponding to lignin and protein appeared more intense in both the susceptible and tolerant groups of rice leaves, while the susceptible group of rice leaves showed significantly stronger spectra corresponding to the polysaccharide region.

DISCUSSION

SR-FTIR microspectroscopy is a powerful technique for identifying the biochemical composition of a sample on the basis of the vibration of the functional groups of the biological molecules. In plant science, SR-FTIR microspectroscopy has been used to analyze and determine the structure and composition of plant tissues such as roots, stems, and leaves (Puttaso et al., 2020). FTIR spectroscopy can be applied to investigate the defense mechanism or interactions between plants and pathogens (Thanh et al., 2017; Thumanu et al., 2017). The fundamental IR bands of

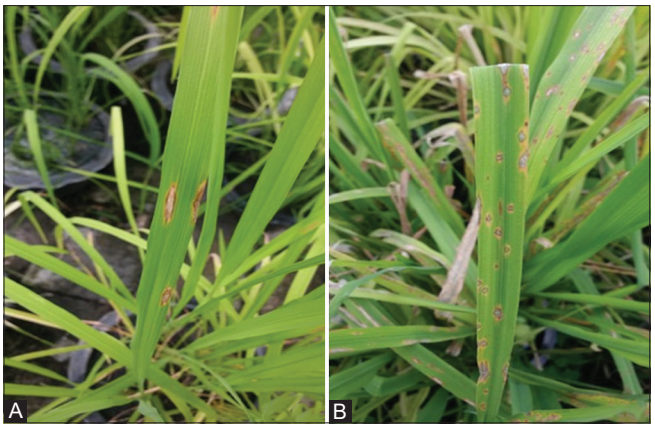

Fig 2. Symptoms of rice blast disease at 14 days after inoculation with *Pyricularia oryzae* pv. *oryzae*. A Resistant cultivar. B Susceptible cultivar.

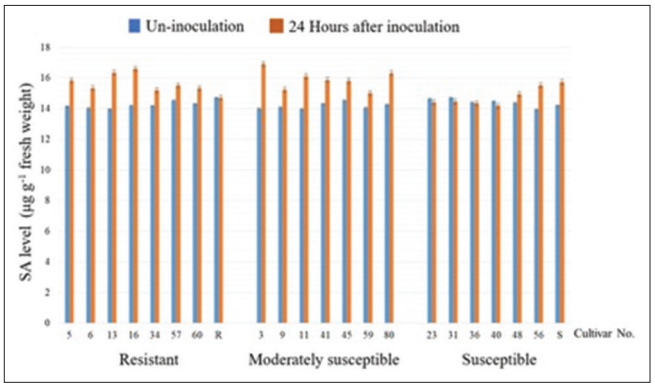

Fig 3. Salicylic acid (SA) accumulation in 22 rice cultivars not inoculated or inoculated with *Pyricularia oryzae* pv. *oryzae* at 24 hours after inoculation under greenhouse conditions.

the functional groups of biomolecules in plant tissues can be measured for protein, lipids, lignin, and polysaccharides (cellulose and hemicellulose). The absorption bands at 3000–2800 cm^{-1} correspond to C-H stretching vibrations from lipids. The vibration of amide I protein at 1650 cm^{-1} consists of 80% C=O and 20% C-N stretching vibrations, whereas the vibration of amide II protein at 1550 cm^{-1} consists of 60% N-H and 40% C-N stretching vibrations (Ji et al., 2020). The band at 1740 cm^{-1} corresponds to the C=O stretching of alkyl esters, which are related to pectin, and the band at 1513 cm^{-1} generally represents lignin. The IR region of polysaccharides associated with the fingerprint region from 1200–900 cm^{-1} is attributed to PO_2^- stretching vibrations C-C, C-O and C-O-C stretching of cellulose and polysaccharide (Kalisz et al., 2021).

The changes of biomolecule after inoculated from the three groups of disease resistant were compared. The result shown that the increasing in protein content (1658 cm^{-1}) of the moderately susceptible and tolerant rice cultivars after inoculation with *P. oryzae* pv. *oryzae* (Figs. 6c and 7c). When the three groups (susceptible, moderately susceptible,

and tolerant) were compared after inoculation, the results showed that the tolerant cultivar presented the greatest protein content, followed by the moderately susceptible and susceptible cultivars (Fig. 9c). These results are in accordance with previous findings, the accumulation of PR proteins in response to disease in tomato and reported that protein synthesis increased in resistant tomato plants infected with pathogens; in contrast, the accumulation level did not increase in susceptible tomato plants. These results could indicate that the pathogen may suppress the levels of defense-related proteins in susceptible plants (Aoun, 2017; Andersen et al., 2018).

Moreover, on the basis of the spectral data, the tolerant and the reference resistant cultivars presented greater amounts of protein than the other groups after inoculation with *P. oryzae* pv. *oryzae* (Fig. 10c). These results suggest that the mechanism of the defense response to *P. oryzae* pv. *oryzae* corresponded to the accumulation of PR proteins. Plant defense-related proteins can interact with plant structure, including the integrity of the cell wall. Several studies have shown that the production of chitinase and glucanase proteins results from induced resistance (Ali et al., 2018). These enzymes are involved in defense reactions against plant pathogens. The immune systems of resistant plants have developed an innate immunity comprising several structural, chemical, and protein-based defenses designed to detect and stop invading organisms as part of an enhanced, long-term, broad-spectrum resistance conferred to plants to defend against future attacks (Miller et al., 2017; Yakura, 2020).

In the defense response of plants, SA acts as a signaling molecule that can induce the expression of PR genes associated with SAR. In rice, SA is a common signal between SA and pathogen responses (Wang and Xiang, 2019). The

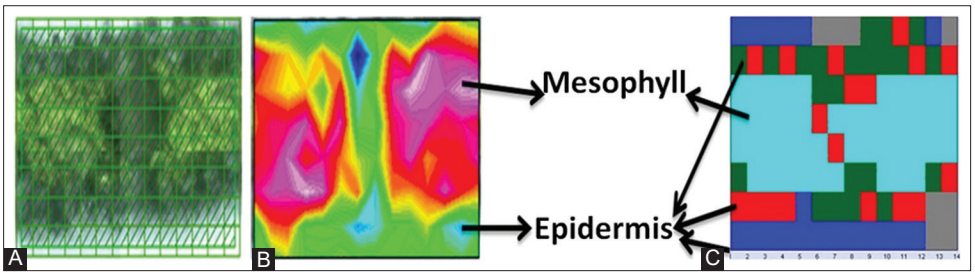

Fig 4. Classification of SR-FTIR microspectroscopy cluster imaging of rice leaves. A Visible image of cross-sections of rice leaves at 36x magnification. B Chemical image obtained from the integrated area under spectrum from 1700–1500 cm^{-1}. C Cluster image derived from an analysis over the regions from 3000–2800 cm^{-1} and 1800–900 cm^{-1}.

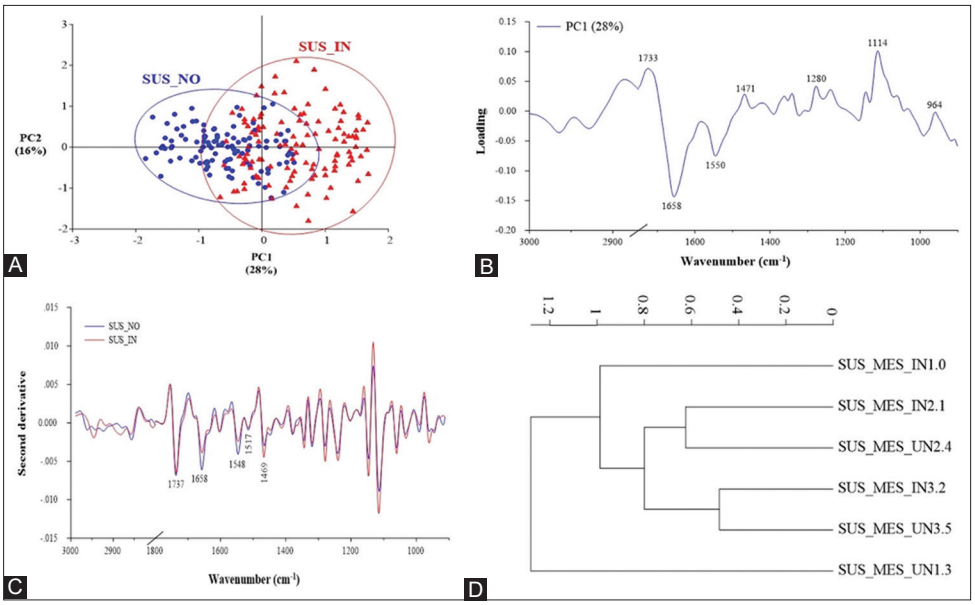

Fig 5. Fourier transform infrared (FTIR) results of a normalized spectral dataset encompassing the wavenumber regions of 3000–2800 cm^{-1} and 1800–900 cm^{-1} from the leaves of susceptible cultivars of rice plants inoculated and not inoculated with *Pyricularia oryzae* pv. *oryzae*. A Principal component analysis (PCA) score plot of two groups of spectra along principal component 1 (PC1). B PC1 correlation loading plot. C Average second-derivative spectra of susceptible cultivars of rice (*Oryza sativa*) plants inoculated and not inoculated with *P. oryzae* pv. *Oryzae*. D Hierarchical cluster analysis (HCA) dendrogram classification of susceptible cultivars of rice plants inoculated and not inoculated with *P. oryzae* pv. *oryzae*.

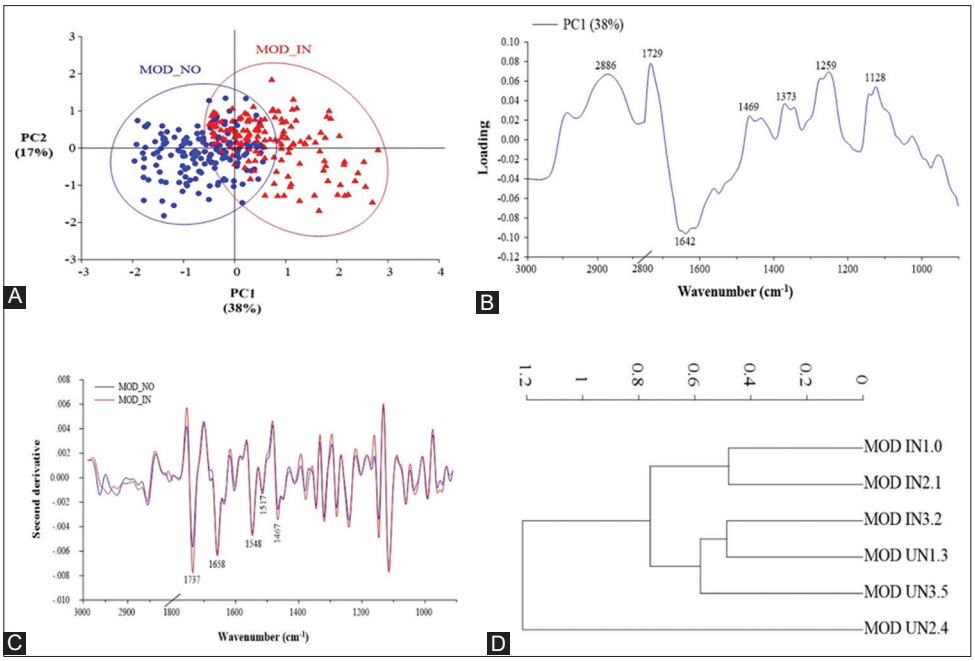

Fig 6. Fourier transform infrared (FTIR) results of the normalized spectral dataset encompassing the wavenumber regions of 3000–2800 cm^{-1} and 1800–900 cm^{-1} of the leaves of moderately susceptible cultivars of rice (*Oryza sativa*) plants inoculated and not inoculated with *Pyricularia oryzae* pv. *oryzae*. A Principal component analysis (PCA) score plot of two groups of spectra along principal component 1 (PC1). B PC1 correlation loading plot. C Average second-derivative spectra of moderately susceptible cultivars of rice (*Oryza sativa*) plants inoculated and not inoculated with *P. oryzae* pv. *Oryzae*. D Hierarchical cluster analysis (HCA) dendrogram classification of moderately susceptible cultivars of rice plants inoculated and not inoculated with *P. oryzae* pv. *oryzae*.

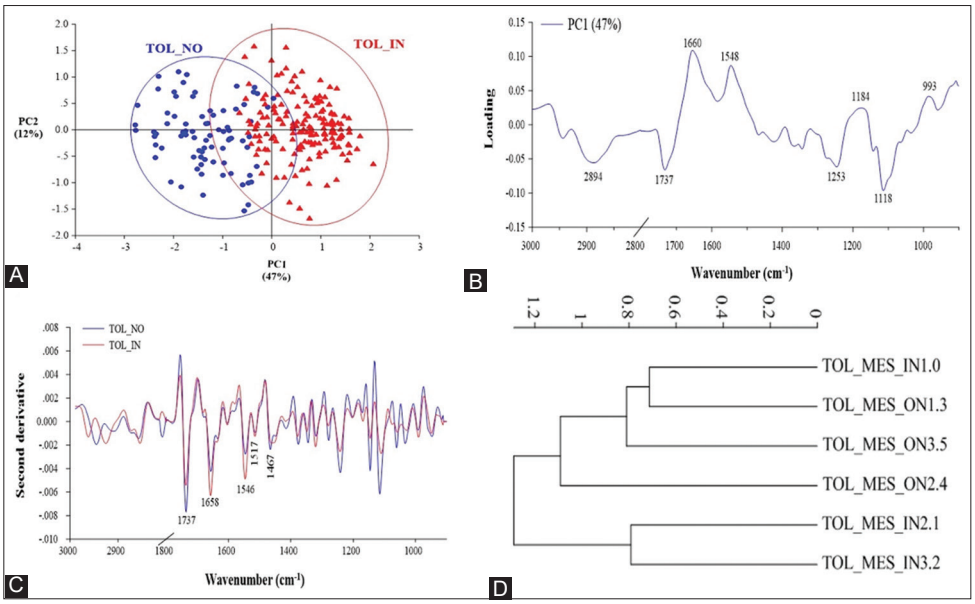

Fig 7. Fourier transform infrared (FTIR) results of the normalized spectral dataset encompassing the wavenumber region of 3000–2800 cm^{-1} and 1800–900 cm^{-1} of the leaves of tolerant cultivars of rice (*Oryza sativa*) plants inoculated and not inoculated with *Pyricularia oryzae* pv. *oryzae*. A Principal component analysis (PCA) score plot of two groups of spectra along principal component 1 (PC1). B PC1 correlation loading plot. C Average second-derivative spectra of tolerant cultivars of rice (*Oryza sativa*) plants inoculated and not inoculated with *P. oryzae* pv. *oryzae*. D Hierarchical cluster analysis (HCA) dendrogram classification of tolerant cultivars of rice plants inoculated and not inoculated with *P. oryzae* pv. *oryzae*.

IR response coincided with increased levels of SA and biological suppression of rice disease, which constitutes an important mechanism for the biological suppression of rice blast disease (Hong et al., 2019). Some researchers studying resistant rice genotypes have reported that the activity of enzymes related to the defense response increased after

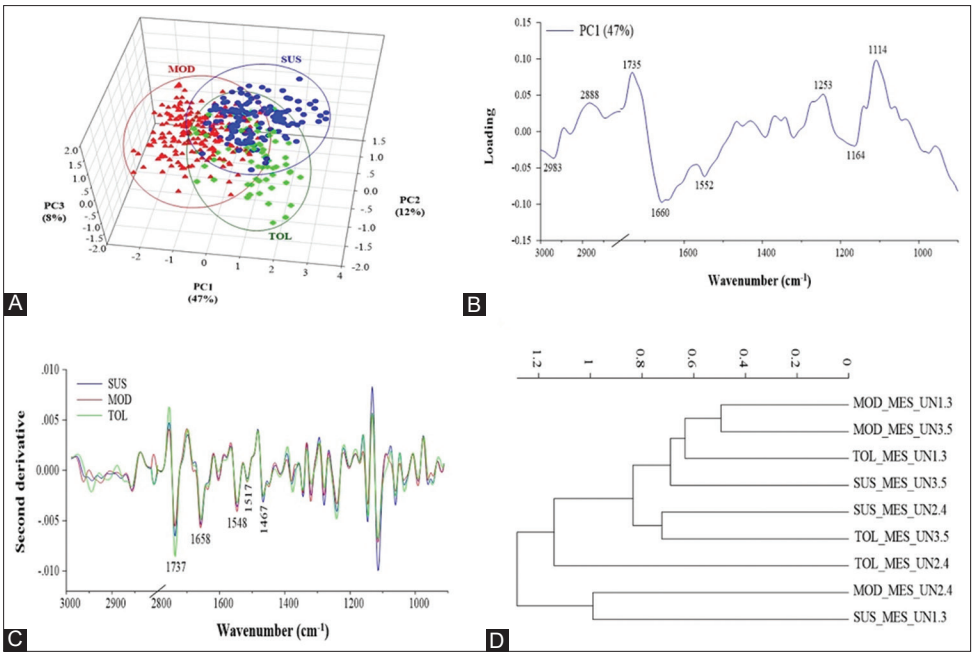

Fig 8. Fourier transform infrared FTIR) results of the normalized spectral dataset encompassing the wavenumber regions of 3000–2800 cm^{-1} and 1800–900 cm^{-1} of the leaves of susceptible, moderately susceptible, and tolerant cultivars of rice (*Oryza sativa*) plants not inoculated with *Pyricularia oryzae* pv. *oryzae*. A Principal component analysis (PCA) score plot of three groups of spectra along principal component 1 (PC1). B PC1 correlation loading plot. C Average second-derivative spectra of susceptible, moderately susceptible, and tolerant cultivars of rice (*Oryza sativa*) plants not inoculated with *P. oryzae* pv. *oryzae*. D Hierarchical cluster analysis (HCA) dendrogram classification of susceptible, moderately susceptible, and tolerant cultivars of rice plants not inoculated with *P. oryzae* pv. *oryzae*.

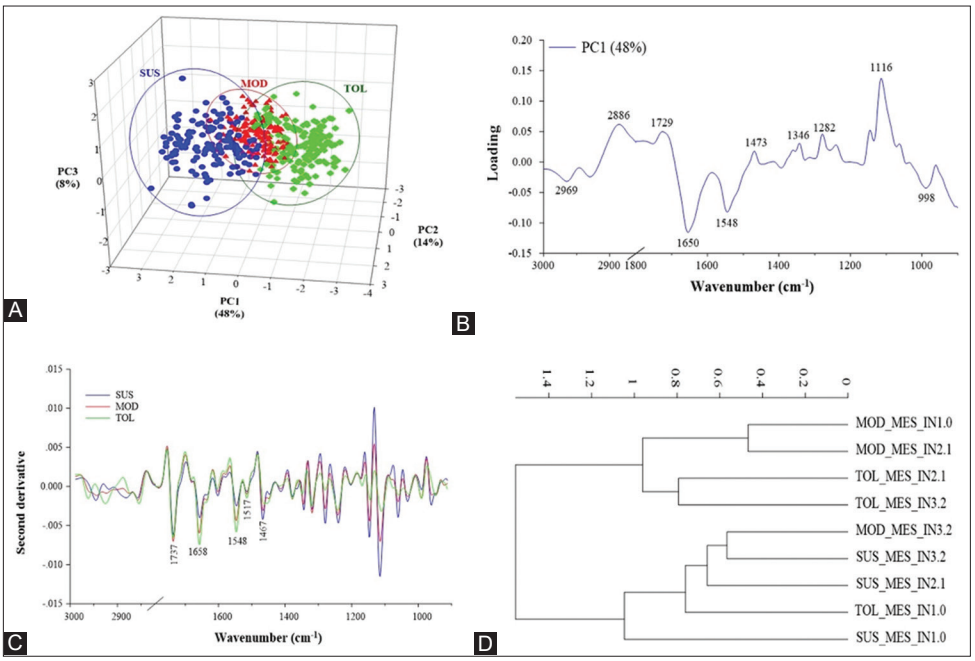

Fig 9. Fourier transform infrared (FTIR) results of the normalized spectral dataset encompassing the wavenumber regions of 3000–2800 cm^{-1} and 1800–900 cm^{-1} of the leaves of susceptible, moderately susceptible, and tolerant cultivars of rice (*Oryza sativa*) plants inoculated with *Pyricularia oryzae* pv. *oryzae*. A Principal component analysis (PCA) score plot of three groups of spectra along principal component 1 (PC1). B PC1 correlation loading plot. C Average second-derivative spectra of susceptible, moderately susceptible, and tolerant cultivars of rice (*Oryza sativa*) plants inoculated with *Pyricularia oryzae* pv. *Oryzae*. D Hierarchical cluster analysis (HCA) dendrogram classification of susceptible, moderately susceptible, and tolerant cultivars of rice plants inoculated with *P. oryzae* pv. *oryzae*.

infection, which might be associated with the defense system (Rossatto et al., 2017). Moreover, interactions between plants and pathogens correlate with PR proteins that act as a defense response against pathogens (Li et al., 2021).

PR proteins compose a diverse group of plant proteins whose expression is induced under pathological conditions. These proteins are toxic to pathogens, and their expression parallels high degrees of pathogen infection and levels of resistance to plant diseases. Furthermore, plants can respond to pathogens by producing reactive oxygen species (ROS) and enzymatic antioxidants. Anushree et al. (2016) studied the response mechanism to disease in different rice cultivars and reported that the expression of PR proteins was induced after infection; these enzymes play a protective role against pathogens more in resistant rice cultivars than in susceptible ones.

The results of biomolecule that correlated with the plant cell wall was compared, the uninoculated tolerant and resistant cultivars presented a relatively high pectin content (1737 cm^{-1}). Furthermore, after inoculation with *P. oryzae* pv. *oryzae*, the moderately susceptible and tolerant cultivars displayed higher lignin (1517 cm^{-1}) and pectin (1737 cm^{-1}) contents than the susceptible and reference sensitive cultivars. These results indicated that lignification is a general mechanism of resistance and occurred in the resistant cultivar of the host plant but not in the susceptible cultivar after infection with the pathogen (Sabella et al., 2018). The role of cell wall modification in response to plant pathogens has been previously reported (Ellis et al., 2002). In response to exposure to pathogens or stress conditions, processes within the plant cell wall may involve an innate immune system; in some instances, these processes can involve Avr proteins via cytoplasmic proteins that are based on a set of plasma membrane-associated proteins that interact with the plant cell wall (Boutrot and Zipfel, 2017; Bacete et al., 2018). Additionally, cellulose is a central component of plant cell walls and can affect many aspects of plant health. Cellulose is synthesized at the plasma membrane by a protein complex (which contains the cellulose synthase protein) that functions specifically in pathogen resistance (Kumar et al., 2017). This enzyme-protein complex is required for cellulose biosynthesis for the primary cell wall and is constitutively activated in response to ET and JA signaling. This process has been detected more in resistant than in wild-type or susceptible plants (Gigli-Bisceglia et al., 2020). Cellulose biosynthesis can be impaired by inducers and inhibitors. By altering the cellulose synthase complex (CSC) of the plasma membrane, inducers can affect cellulose biosynthesis, which leads to irregular production of JA, ROS, lignin, and pectin resulting in the activation of the disease response (Tobias et al., 2020; Wang et al., 2020). However, plants can exhibit a decrease in

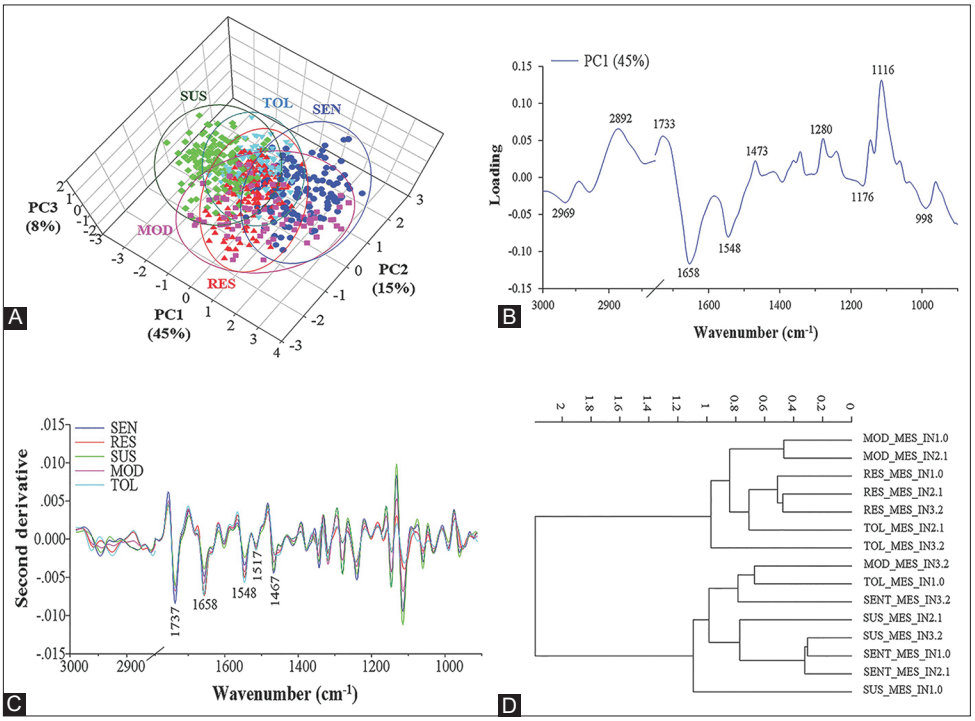

Fig 10. Fourier transform infrared (FTIR) results of the normalized spectral dataset encompassing the wavenumber regions of 3000–2800 cm^{-1} and 1800–900 cm^{-1} of the leaves of susceptible, moderately susceptible, and tolerant rice (*Oryza sativa*) cultivars compared with the reference sensitive and resistant cultivars inoculated with *Pyricularia oryzae* pv. *oryzae*. A Principal component analysis (PCA) score plot of five groups of spectra along principal component 1 (PC1). B PC1 correlation loading plot. C Average second-derivative spectra of susceptible, moderately susceptible, and tolerant cultivars as well as the sensitive and resistant reference cultivars of rice plants inoculated with *P. oryzae* pv. *oryzae*. D Hierarchical cluster analysis (HCA) dendrogram classification of susceptible, moderately susceptible, tolerant, sensitive and resistant cultivars of rice plants inoculated with *P. oryzae* pv. *oryzae*.

cellulose biosynthesis activity because of pathogens. Plants use cell walls as an active defensive barrier against inducers or pathogens such as bacteria, fungi, oomycetes, insects, and nematodes as well as against abiotic stresses such as drought, cold, and heat. Nevertheless, after infection, elicitors are sometimes released from pathogens, triggering signaling cascades to activate defense responses.

Sugar content was also noted to increase to 1450 cm^{-1} and 1420 cm^{-1} in the tolerant cultivars after inoculation with *P. oryzae* pv. *oryzae*. High levels of total sugars occur as a mechanism of disease resistance. Nutritional utilization of sugars by invading pathogens has been previously reported. Compared with to resistant genotypes, disease development in susceptible genotypes was found to be associated with significant reductions in total sugar contents. These results corroborate the findings of other researchers who reported that resistant wheat genotypes that presented increased amounts of total sugars in response to infection. Sugars act as precursors for the synthesis of phenolics, phytoalexins, lignin, and cellulose, which play important roles in the defense response of plants against pathogens (Chaliha et al., 2018; Choudhury et al., 2018; Panda and Barik, 2021).

The results of our study suggest that the variation in biochemical components of rice plants was altered after pathogen infection. When the susceptible, moderately susceptible, and tolerant cultivars were compared, variation in the biochemical components of rice tissues was detected. This variation may be correlated with the plant defense response to disease. In addition, we demonstrated that the SR-FTIR microspectroscopy technique can be used to explain the primary mechanisms of the defense response via differences in peak intensities of biochemical components within the groups of disease resistant rice plant tissue.

CONCLUSIONS

Screening rice blast-resistant cultivars via SR-FTIR microspectroscopy revealed biochemical component differences in rice tissues, which may correlate with plant-defense responses to disease. The rice leaf tissue is known to protect against plant- pathogenic fungi. Resistant group has a high level of biochemical composition that related to disease defense such as proteins, pectin and lignin. As a result, resistant rice cultivars have a low level of disease severity. This technique could be used in the classification of disease resistance in rice leaf tissue. Tolerant rice plants produced high content of pectin and lignin before inoculated, which was not seen in the susceptible and moderate plants. Furthermore, the mechanism of disease defense in the tolerant showed higher content of protein than in the susceptible and moderately susceptible that relate to disease defence. The mechanism responsible to pathogen based biochemical changes of susceptible, moderately susceptible, and tolerant were different. However, selection of resistant-rice cultivars may improve breeding programs.

ACKNOWLEDGMENTS

We wish to express our special thanks to the National Research Council of Thailand (NRCT) for providing funding (Grant No. 3/2560) and to the Sakon Nakhon Rice Research Center for providing the rice seed, and we gratefully acknowledge Scott Dworak, M.Sc., for his assistance with English language editing.

CONFLICT OF INTEREST

The authors declare that they have no conflict of interest.

Authors' contributions

Piyaporn Phansak, Supatcharee Siriwong, Rungthip Sangpueak, Nantawan Kanawapee, Kanjana Thumanu, and Natthiya Buensanteai contributed to the research conception and design. Piyaporn Phansak, Supatcharee Siriwong, Rungthip Sangpueak prepared the materials and collected the analyzed data. Supatcharee Siriwong and Kanjana Thumanu performed the deep SR-FTIR rice blast screening and analyzed data. Piyaporn Phansak and Rungthip Sangpueak Supatcharee Siriwong performed the statistical analysis and drafted the manuscript. Piyaporn Phansak, Natthiya Buensanteai and Nantawan Kanawapee commented on and edited previous versions of the manuscript. All authors have read and approved the final manuscript.

REFERENCES

Ali, S., B. A. Ganaib, A. N. Kamilib, A. A. Bhat, Z. A. Mir, J. A. Bhat, A. Tyagi, S. T. Islam, M. Mushtaq, P. Yadav, S. Rawat and A. Grover. 2018. Pathogenesis-related proteins and peptides as promising tools for engineering plants with multiple stress tolerance. Microbiol. Res. 212-213: 29-37.

Alonso-Simón, A., P. García-Angulo, H. Mélida, A. Encina, J. M. Álvarez and J. L. Acebes. 2011. The use of FTIR spectroscopy to monitor modifications in plant cell wall architecture caused by cellulose biosynthesis inhibitors. Plant Signal. Behav. 6: 1104-1110.

Andersen, E. J., S. Ali, E. Byamukama, Y. Yen and M. P. Nepal. 2018. Disease Resistance Mechanisms in Plants. Genes. 9: 339.

Anushree, P. U., R. M. Naik, R. D. Satbhai, A. P. Gaikwad and C. A. Nimbalkar. 2016. Differential biochemical response of rice (*Oryza sativa* L.) genotypes against rice blast (*Magnaporthe oryzae*). Cogent. Biol. 2: 1264162.

Aoun, M. 2017. Host defense mechanisms during fungal pathogenesis and how these are overcome in susceptible plants: A review. Int.

J. Bot. 13: 82-102.

Ashkani, S., M. Y. Rafii, M. Shabanimofrad, G. Miah, M. Sahebi, P. Azizi, F. A. Tanweer, M. S. Akhtar and A. Nasehi. 2015. Molecular breeding strategy and challenges towards improvement of blast disease resistance in rice crop. Front. Plant Sci. 6: 886.

Asibi, A. E., Q. Chai and J. A. Coulter. 2019. Rice blast: A disease with implications for global food security. Agronomy. 9: 451.

Bacete, L., H. Mélida, E. Miedes and A. Molina. 2018. Plant cell wall-mediated immunity: Cell wall changes trigger disease resistance responses. Plant J. 93: 614-636.

Backer, R., S. Naidoo and N. V. D. Berg. 2019. The nonexpressor of pathogenesis-related genes 1 (*npr1*) and related family: mechanistic insights in plant disease resistance. Front. Plant Sci. 10: 102.

Bernacki, M. J., A. Rusaczonek, W. Czarnocka and S. Karpi´nski. 2021. Salicylic acid accumulation controlled by LSD1 is essential in triggering cell death in response to abiotic stress. Cells. 10: 962.

Bigini, V., F. Camerlengo, E. Botticella, F. Sestili and D. V. Savatin. 2021. Biotechnological resources to increase disease-resistance by improving plant immunity: A sustainable approach to save cereal crop production. Plants. 10: 1146.

Boutrot, F. and C. Zipfel. 2017. Function, discovery, and exploitation of plant pattern recognition receptors for broad-spectrum disease resistance. Ann. Rev. Phytopathol. 55: 257-286.

Brzozowski, L. and M. Mazourek. 2018. A sustainable agricultural future relies on the transition to organic agroecological pest management. Sustainability. 10: 2023.

Brodersen, P., F. G. Malinovsky, K. Hématy, M. A. Newman and J. Mundy. 2005. The role of salicylic acid in the induction of cell death in *Arabidopsis* acd11. Plant Physiol. 138: 1037-1045.

Buitrago, M., A. K. Skidmore, T. A. Groen and C. A. Hecker. 2018. Connecting infrared spectra with plant traits to identify species. ISPRS J. Photogramm Remote. Sens. 139: 183-200.

Cao, Z., Z. Wang, Z. Shang and J. Zhao. 2017. Classification and identification of *Rhodobryum roseum* Limpr. and its adulterants based on fourier-transform infrared spectroscopy (FTIR) and chemometrics. PLoS One. 12: e0172359.

Chaliha, C., M. D. Rugen, R. A. Field and E. Kalita. 2018. Glycans as modulators of plant defense against filamentous pathogens. Front. Plant Sci. 9: 928.

Choudhury, S., H. Hu, P. Larkin, H. Meinke, S. Shabala, I. Ahmed and M. Zhou. 2018. Agronomical, biochemical and histological response of resistant and susceptible wheat and barley under BYDV stress. Peer. J. 6: e4833.

Devanna, N. B., J. Vijayan and T. R. Sharma. 2014. The blast resistance gene Pi54 of cloned from *Oryza officinalis* interacts with Avr-Pi54 through its novel non-LRR domains. PLoS One. 9: e104840.

Desmedt, W., W. Jonckheere, V. H. Nguyen, M. Ameye, N. D. Zutter, K. D. Kock, J. Debode, T. V. Leeuwen, K. Audenaert, B. Vanholme and T. Kyndt. 2021. The phenylpropanoid pathway inhibitor piperonylic acid induces broad-spectrum pest and disease resistance in plants. Plant Cell Environ. 2021: 1-18.

Disthaporn, S. 1994. Current rice blast epidemics and their management in Thailand. In: R. S. Zeigler, S. A., Leong and P. S. Teng (Eds.), Rice Blast Disease. CAB International, Wallingford, pp. 333-342.

Dinant, S., N. Wolff, F. De Marco, F. Vilaine, L. Gissot, E. Aubry, C. Sandt, C. Bellini and R. Le Hir. 2019. Synchrotron FTIR and Raman spectroscopy provide unique spectral fingerprints for *Arabidopsis* floral stem vascular tissues. J. Exp. Bot. 70: 871-884.

Durak, T. and J. Depciuch. 2020. Effect of plant sample preparation and measuring methods on ATR-FTIR spectra results. Environ. Exp. Bot. 169: 103915.

Dong, O. X. and P. C. Ronald. 2019. Genetic engineering for disease resistance in plants: recent progress and future perspectives. Plant Physiol. 180: 26-38.

Ellis, C., I. Karafyllidis, C. Wasternack and J. G. Turner. 2002. The *Arabidopsis* mutant cev1 links cell wall signaling to jasmonate and ethylene responses. Plant Cell. 14: 1557-1566.

Erb, M. and D. J. Kliebenstein. 2020. Plant secondary metabolites as defenses, regulators, and primary metabolites: The blurred functional trichotomy. Plant Physiol. 184: 39-52.

Filgueiras, C. C., A. D. Martins, R. V. Pereira and D. S. Willett. 2019. The ecology of salicylic acid signaling: Primary, secondary and tertiary effects with applications in agriculture. Int. J. Mol. Sci. 20: 5851.

Forouhar, F., Y. Yang, D. Kumar, Y. Chen, E. Fridman, S. W. Park, Y. Chiang, T. B. Acton, G. T. Montelione, E. Pichersky, D. F. Klessig and L. Tong. 2005. Structural and biochemical studies identify tobacco SABP2 as a methyl salicylate esterase and implicate it in plant innate immunity. Proc. Natl. Acad. Sci. U. S. A. 102: 1773-1778.

Gigli-Bisceglia, N., T. Engelsdorf and T. Hamann. 2020. Plant cell wall integrity maintenance in model plants and crop species-relevant cell wall components and underlying guiding principles. Cell. Mol. Life Sci. 77: 2049-2077.

Gierlinger, N. 2017. New insights into plant cell walls by vibrational microspectroscopy. Appl. Spectrosc. Rev. 53: 517-551.

Goff, K. L., T. H. Ellis and K. E. Wilson. 2019. Synchrotron FTIR as a tool for studying populations and individual living cells of green algae. bioRxiv. 808220: 1-25.

Haggag, W. M., M. M. Hussein, M. M. Tawfik and S. F. El Habbasha. 2014. Enhancement of wheat resistant to diseases by elicitors. Int. J. Sci. Res. 3: 1526-1530.

Hong, Y., Q. Liu, Y. Cao, Y. Zhang, D. Chen, X. Lou, S. Cheng and L. Cao. 2019. The OsMPK15 negatively regulates *Magnaporthe oryza* and Xoo disease resistance via SA and JA signaling pathway in rice. Front. Plant Sci. 10: 752.

Huang, H., F. Ullah, D. X. Zhou, M. Yi and Y. Zhao. 2019. Mechanisms of ROS regulation of plant development and stress responses. Front. Plant Sci. 10: 800.

Huang, T. Y., S. G. Li, Y. P. Wang and H. Y. Li. 2003. Accelerated improvement of bacterial blight resistance of 'Shuhui 527' using molecular marker-assisted selection. Chin. J. Biotechnol. 19: 153-157.

Isah, T. 2019. Stress and defense responses in plant secondary metabolites production. Biol. Res. 52: 39.

Janda, T., G. Szalai and M. Pál. 2020. Salicylic acid signaling in plants. Int. J. Mol. Sci. 21: 2655.

Ji, Y., X. Yang, Z. Ji, L. Zhu, N. Ma, D. Chen, X. Jia, J. Tang and Y. Cao. 2020. DFT-calculated IR spectrum amide I, II, and III band contributions of N-methylacetamide fine components. ACS Omega. 5: 8572-8578.

Jiang, C. J., M. Shimono, S. Sugano, M. Kojima, K. Yazawa, R. Yoshida, H. Inoue, N. Hayashi, H. Sakakibara and H. Takatsuji. 2010. Abscisic acid interacts antagonistically with salicylic acid signaling pathway in rice-*Magnaporthe grisea* interaction. Mol. Plant Microbe. Interact. 23: 791-798.

Jiang, N., J. Yan, Y. Liang, Y. Shi, Z. He, Y. Wu, Q. Zeng, X. Liu and J. Peng. 2020. Resistance genes and their interactions with bacterial blight/leaf streak pathogens (*Xanthomonas oryzae*) in rice (*Oryza sativa* L.) an updated review. J. Rice Pest. Sci. 13: 3.

Kalisz, G., B. Gieroba, O. Chrobak, M. Suchora, A. L. Starosta and

A. Sroka-Bartnicka. 2021. Vibrational spectroscopic analyses and imaging of the early middle ages hemp bast fibres recovered from lake sediments. Molecules. 26: 1314.

Kongcharoen, N., N. Kaewsalong and T. Dethoup. 2020. Efficacy of fungicides in controlling rice blast and dirty panicle diseases in Thailand. Sci. Rep. 10: 16233.

Kumar, M., I. Atanassov and S. Turner .2017. Functional analysis of cellulose synthase (CESA) protein class specificity. Plant Physiol. 173: 970-983.

Kwanwah, M. R., T. WongSa, T. Monkham, S. Chankaew and J. Sanitchon. 2020. Large scale screening for blast resistance of Thai indigenous lowland rice germplasm. Khon Kaen Agric. J. 48: 441-452.

Lang, C. E., J. R. Macdonald, D. S. Reisman, L. Boyd, L. Boyd, T. J. Kimberley, S. M. Schindler-Ivens, T. G. Hornby, S. A. Ross and P. L. Scheets. 2009. Observation of amounts of movement practice provided during stroke rehabilitation. Arch. Phys. Med. Rehabil. 90: 1692-1698.

Lahlali, R., S., Kumar, L. Wang, L. Forseille, N. Sylvain, M. Korbas, D. Muir, G. Swerhone, J. R. Lawrence, P. R. Fobert, G. Peng and C. Karunakaran. 2016. Cell wall biomolecular composition plays a potential role in the host Type II resistance to Fusarium head blight in wheat. Front. Microbiol. 7: 910.

Lefevere, H., L. Bauters and G. Gheysen. 2020. Salicylic acid biosynthesis in plants. Front. Plant Sci. 11: 338.

Lee, S. W., R. N. Nazar, D. A. Powell and J. Robb. 1992. Reduced *PAL* gene suppression in *Verticillium*-infected resistant tomatoes. Plant. Mol. Biol. 18: 345-352.

Li, N., X. Han, D. Feng, D. Yuan and L-J. Huang. 2019. Signaling crosstalk between salicylic acid and ethylene/jasmonate in plant defense: do we understand what they are whispering? Int. J. Mol. Sci. 20: 671.

Li, S., Z. Wang, B. Tang, L. Zheng, H. Chen, X. Cui, F. Ge and D. Liu. 2021. A pathogenesis-related protein-like gene is involved in the *Panax notoginseng* defense response to the root rot pathogen. Front. Plant Sci. 11: 610176.

Loladze, A., F. A. Rodrigues, F. Toledo, F. S. Vicente, B. Gérard and M. P. Boddupalli. 2019. Application of remote sensing for phenotyping tar spot complex resistance in maize. Front. Plant Sci. 10: 552.

Miller, R. N. G., G. S. C. Alves and M. A. V. Sluys. 2017. Plant immunity: Unravelling the complexity of plant responses to biotic stresses. Ann. Bot. 119: 681-687.

Panda, D. and J. Barik. 2021. Flooding tolerance in rice: Focus on mechanisms and approaches. Rice Sci. 28: 43-57.

Parinthawong, N., P. Tansian and T. Sreewongchai. 2015. Genetic mapping of leaf blast resistance gene in landrace rice cultivar “GS19769”. Maejo. Int. J. Sci. Technol. 9: 278-287.

Pei, Y. F., Q. Z. Zhang, Z. T. Zuo and Y. Z. Wang. 2018. Comparison and identification for rhizomes and leaves of *Paris yunnanensis* based on Fourier transform mid-infrared spectroscopy combined with chemometrics. Molecules. 23: 3343.

Petit-Houdenot, Y. and I. Fudal. 2017. Complex interactions between fungal avirulence genes and their corresponding plant resistance genes and consequences for disease resistance management. Front. Plant Sci. 8: 1072.

Poonsin, R. and N. Parinthawong. 2020. Investigation of rice blast resistant genes in Thai elite rice varieties (*Oryza sativa* L.) for improvement of broad-spectrum blast disease resistance variety. Int. J. Agric. Technol. 16: 109-118.

Puttaso, P., W. Namanusart, K.Thumanu, B. Kamolmanit, A. Brauman and P. Lawongsa. 2020. Assessing the effect of rubber (*Hevea brasiliensis* (Willd. ex A. Juss.) Muell. Arg.) leaf chemical composition on some soil properties of differently.

Raskin, I., I. M. Turner and W. R. Melander. 1989. Regulation of heat production in the inflorescence of an *Arum* lily by endogenous salicylic acid. Proc. Natl. Acad. Sci. U. S. A. 86: 2214-2218.

Rijal, T. R., G. B. Hamal, P. Jha and K. B. Koirala. 2017. Identification of resistant genotypes on rice against blast disease under field condition at Rampur, Chitwan. Int. J. Appl. Sci. Biotechnol. 5: 505-510.

Rosi, F., L. Cartechini, D. Sali and C. Miliani. 2019. Recent trends in the application of Fourier transform infrared (FT-IR) spectroscopy in heritage science: From micro-to non-invasive FT-IR. Phys. Sci. Rev. 4: 1-10.

Rossatto, T., M. N. D. Amaral, L. C. Benitez, I. L. Vighi, E. J. B. Braga, A. M. D. M. Júnior, M. A. C. Maia and L. D. S. Pinto. 2017. Gene expression and activity of antioxidant enzymes in rice plants, cv. BRS AG, under saline stress. Physiol. Mol. Biol. Plants. 23: 865-875.

Sabella, E., A. Luvisi, A. Aprile, C. Negro, M. Vergine, F. Nicolì, A. Miceli and L. D. Bellis. 2018. *Xylella fastidiosa* induces differential expression of lignification related-genes and lignin accumulation in tolerant olive trees cv. Leccino. J. Plant Physiol. 220: 60-68.

Sharma, S., A. Mustafiz, S. L. Singla-Pareek, P. S. Srivastava and S. K. Sopory. 2012. Characterization of stress and methylglyoxal inducible triose phosphate isomerase (OscTPI) from rice. Plant Signal. Behav. 7: 1337-1345.

Straub, C. S., J. A. Faselt, E. S. Keyser and M. Traugott. 2020. Host plant resistance promotes a secondary pest population. Ecosphere. 11: e03073.

Staniszewska-Ślęzak, E., A. Fedorowicz, K. Kramkowski, A. Leszczynska, S. Chlopicki, M. Baranska and K. Malek. 2015. Plasma biomarkers of pulmonary hypertension identified by Fourier transform infrared spectroscopy and principal component analysis. Analyst. 140: 2273-2279.

Straková, P., T. Larmola, J. Andrés, N. Ilola, P. Launiainen, K. Edwards, K. Minkkinen and R. Laiho 2020. Quantification of plant root species composition in peatlands using FTIR spectroscopy. Front. Plant Sci. 11: 597.

Thanh, T. L., K. Thumanu, S. Wongkaew, N. Boonkerd, N. Teaumroong, P. Phansak and N. Buensanteai. 2017. Salicylic acid-induced accumulation of biochemical components associated with resistance against *Xanthomonas oryzae* pv. *oryzae* in rice. J. Plant Interact. 12: 108-120.

Thepbandit, W., N. K. Papathoti, J. R. Daddam, K. Thumanu, S. Siriwong, T. L. Thanh and N. Buensanteai. 2021. Identification of salicylic acid mechanism against leaf blight disease in *Oryza sativa* by SR-FTIR microspectroscopic and docking studies. Pathogens. 10: 652.

Thumanu, K., D. Wongchalee, M. Sompong, P. Phansak, T. Le Thanh, W. Namanusart, K. Vechklang, S. Kaewnum and N. Buensanteai. 2017. Synchrotron-based FTIR microspectroscopy of chili resistance induced by *Bacillus subtilis* strain D604 against anthracnose disease. J. Plant Interact. 12: 255-263.

Tobias, L. M., A.V. Spokevicius, H. E. McFarlane and G. Bossinger. 2020. The cytoskeleton and its role in determining cellulose microfibril angle in secondary cell walls of woody tree species. Plants. 9: 90.

Turaidar, V., M. Reddy, R. Anantapur, K. N. Krupa, N. Dalawai, C. A. Deepak and H. K. M. Kumar. 2018. Screening of traditional rice varieties (TRVs) for

TÜrker-kaya, S. and C. W. Huck. 2017. A review of mid-infrared and near-infrared imaging: Principles, concepts and applications in

plant tissue analysis. Molecules. 22: 168.

Vasudevan, B., C. Esposito, C. Peterson, C. Coronado and K. J. Ciuffreda. 2014. Under-correction of human myopia is it myopigenic: A retrospective analysis of clinical refraction data. J. Optom. 7: 147-152.

Wang, P. and M. Xiang. 2019. Research Progress of NPR Genes in Signal Pathway of Salicylic Acid Mediated Plant Disease Resistance. E3S Web of Conferences, No. 145, 01038.

Wang, L., B. E. H. G. A. Khan, E. R. Cruz, S. Persson1 and I. S. Wallace. 2020. Associations between phytohormones and cellulose biosynthesis in land plants. Ann. Bot. 126: 807-824.

War, A. R., M. G. Paulraj, M. Y. War and S. Ignacimuthu. 2011. Role of salicylic acid in induction of plant defense system in chickpea (*Cicer arietinum* L.). Plant Signal. Behav. 6(11): 1787-1792.

Wopereis, S., C. M. Rubingh, M. J. van Erk, E. R. Verheij, T. van Vliet, N. H. P. Cnubben, A. K. Smilde, J. van der Greef, B. van Ommen and H. F. J. Hendriks. 2009. Metabolic profiling of the response to an oral glucose tolerance test detects subtle metabolic changes. PLoS One. 4: e4525.

Wu, Z., Y. Huang, Y. Li, J. Dong, X. Liu and C. Li. 2019. Biocontrol of *Rhizoctonia solani* via induction of the defense mechanism and antimicrobial compounds produced by *Bacillus subtilis* SL-44 on pepper (*Capsicum annuum* L.). Front. Microbiol. 10: 2676.

Wu, Z., G. Wang, B. Zhang, T. Dai, A. Gu, X. Li, X. Cheng, P. Liu, J. Hao and X. Liu. 2021. Metabolic mechanism of plant defense against rice blast induced by probenazole. Metabolites. 11: 246.

Yakura, H. 2020. Cognitive and memory functions in plant immunity. Vaccines. 8: 541.

Zhang, S., J. Liu, B. Xu and J. Zhou. 2021. Differential responses of *Cucurbita pepo* to *Podosphaera xanthii* reveal the mechanism of powdery mildew disease resistance in pumpkin. Front. Plant Sci. 12: 633221.